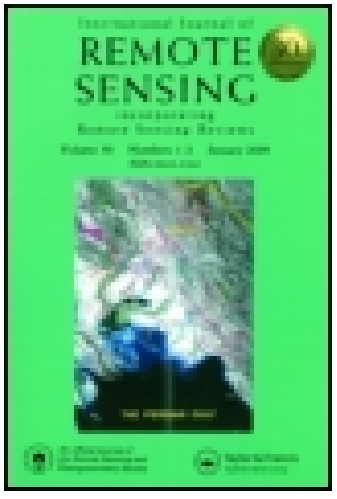


International Journal of Remote Sensing

Publication details, including instructions for authors and subscription information:
http://www.tandfonline.com/loi/tres20

# Retrieving and broadcasting near-real-time biophysical parameters from MODIS and SEVIRI receiving stations at the global change unit of the University of Valencia

Y. Julien[a], J. A. Sobrino[a] & G. Sòria[a]

[a] Global Change Unit, Image Processing Laboratory, Scientific Park, University of Valencia, 46980 Paterna, Spain

Published online: 29 Jun 2015.

*International Journal of Remote Sensing*, 2015
http://dx.doi.org/10.1080/01431161.2015.1040134

Taylor & Francis
Taylor & Francis Group

# Retrieving and broadcasting near-real-time biophysical parameters from MODIS and SEVIRI receiving stations at the global change unit of the University of Valencia

Y. Julien*, J. A. Sobrino, and G. Sòria

*Global Change Unit, Image Processing Laboratory, Scientific Park, University of Valencia, 46980 Paterna, Spain*

(*Received 26 November 2014; accepted 23 January 2015*)

We present here the automatic processing chains implemented at the Global Change Unit of the University of Valencia. These allow for a near-real-time retrieval of various biophysical parameters from both Sun-synchronous TERRA/AQUA Moderate Resolution Imaging Spectroradiometer (MODIS) and geostationary Meteosat Second Generation Spinning Enhanced Visible and Infrared Imager (MSG SEVIRI) sensors. Retrieved parameters, namely sea and land surface temperatures (SST and LST, respectively), normalized difference vegetation index (NDVI), and vegetation condition index (VCI), are similar for both sensors, and specific approaches have been developed and implemented for near-real-time parameter retrievals: <2 hours for MODIS and <5 min for MSG SEVIRI. Bidirectional reflectance distribution function (BRDF) correction is still required to be implemented in both processing chains, while more advanced parameters are already retrieved (hot spot detection and MSG SEVIRI phenology), in good agreement with independent ground observations. Validation of the retrieved products is underway and the above-mentioned products are available for downloading at http://ceosspain.lpi.uv.es.



## 1. Introduction

With an ever increasing number of satellites orbiting our planet, the amount of data available for Earth observation is rapidly growing. However, due to the amount of data processed, official repositories for remotely sensed biophysical products do not usually provide a near-real-time access to these data.

Within the framework of the Spanish CEOS-SPAIN project, a processing and broadcasting scheme has been developed and implemented at the Global Change Unit of the University of Valencia, taking advantage of the receiving Moderate Resolution Imaging Spectroradiometer (MODIS) and Meteosat Second Generation Spinning Enhanced Visible and Infrared Imager (MSG SEVIRI) stations. The processing scheme has been designed with the goal of near-real-time processing of the data, estimating biophysical parameters as straightforwardly as possible. The selected parameters for estimation are the following: sea and land surface temperatures (SST and LST, respectively), for which the total amount of water vapour (WV) and emissivities are needed; normalized difference vegetation index (NDVI); and vegetation condition index (VCI). However, different corrections are needed for accurate retrieval of these parameters, such as atmospheric correction and bidirectional reflectance distribution function (BRDF) correction for visible bands.

*Corresponding author. Email: yves.julien@uv.es

This article presents in detail the data received by the MODIS and MSG SEVIRI stations located at the Global Change Unit, as well as the processing chain for MODIS and MSG SEVIRI data. Finally, a few applications of these data are presented.

## 2. Data

Two different streams of data are received at the Global Change Unit, from MSG SEVIRI and MODIS platforms. SEVIRI data are provided by the MSG geostationary platform, at 3 km resolution at nadir, with an image every 15 min, amounting to 21 GB/day before processing. This sensor acquires 11 bands, of which two are located in the visible and near-infrared wavelengths (Vis06 and Vis08), two located in the middle infrared wavelengths (Ir016 and Ir039), and seven located in the 6–14 μm thermal infrared spectral region (Wv062, Wv073, Ir087, Ir097, Ir108, Ir120, and Ir134), where the number indicates the central wavelength (to be multiplied by 100 nm).

MODIS data are Sun-synchronous, with around three overpasses during the day and three during the night, amounting to 4 GB/day before processing. The MODIS instrument provides data in 36 spectral bands ranging in wavelength from 0.4 to 14.4 μm. Two bands are imaged at a nominal resolution of 250 m at nadir (visible and near-infrared wavelengths), with five bands at 500 m (visible to middle infrared) and the remaining 29 at 1 km (middle to thermal infrared).

MODIS data consist of the satellite overpasses within reach of the antenna located at the University of Valencia, overpasses which cover most of Western Europe, while SEVIRI data consist of the entire hemisphere centred on the (0,0) latitude and longitude point. Figure 1 presents quicklooks for both MODIS and SEVIRI single acquisitions. MODIS quicklook (Figure 1(*a*)) is a Red–Green–Blue (RGB) composite, with bands 1, 4, and 3 coded as R, G, and B, respectively, for daytime acquisitions, while for night-time acquisitions a greyscale image of thermal band 31 is used (not shown). As a result, vegetation appears in MODIS quicklook as green, clouds as white, and sand as yellow. SEVIRI quicklook (Figure 1(*b*)) is also an RGB composite, with bands IR108, Vis06, and Vis08 coded as R, G, and B, respectively. Therefore, high-temperature areas appear as red, vegetation as green, and clouds as light blue.

Each data stream is received respectively on a dedicated computer and then processed by another dedicated computer, finally to be uploaded to a common server. A web of control routines between computers allows for the early detection of any reception, processing, or archiving failures.

## 3. MODIS processing

Both MODIS and MSG SEVIRI streams of data are processed linearly following a similar scheme (see Table 1). The selected algorithms for MODIS processing were chosen from a literature review and are based on standard procedures, such as contextual fire detection (Mod14; Giglio et al. 2003); Mod35 cloud screening (Ackerman et al. 2010); Simplified Method for Atmospheric Correction (SMAC; Rahman and Dedieu 1994), completed using specific methods described briefly below. Characteristics (resolution, average sample size, etc.) of each of the products described hereafter are presented in Table 2.

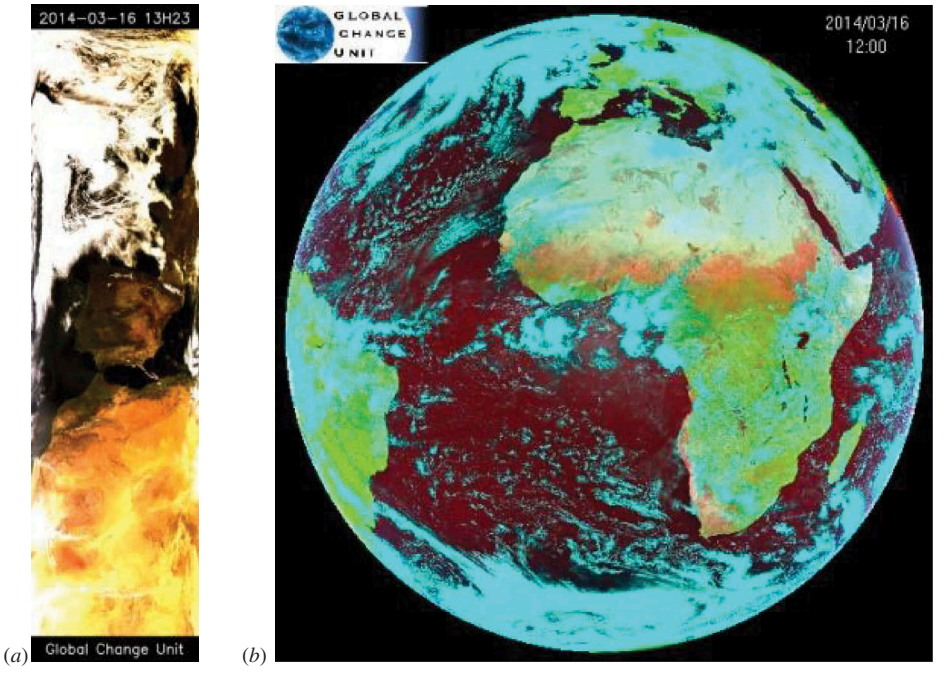


(*a*) (*b*)

Figure 1. MODIS (*a*) and SEVIRI (*b*) quicklooks of received data at the Global Change Unit of the University of Valencia. MODIS quicklook is a Red–Green–Blue (RGB) composite with bands 1, 4, and 3, while SEVIRI RGB quicklook uses bands IR108, Vis06, and Vis08. See text for details.

Table 1. Description of the processing chain and products retrieved from both MODIS and MSG SEVIRI data streams. Products in bold type are available for download from CEOS-SPAIN online geo-portal: http://ceosspain.lpi.uv.es.

| Processing step | MODIS | MSG SEVIRI |
|---|---|---|
| Data unpacking and calibrating | Yes | Yes |
| Geolocation | Yes | No |
| Hot spot detection | Mod14 (Giglio et al. 2003) | Calle, Casanova, and Romo (2006) |
| Cloud detection | **Mod35 (Ackerman et al. 2010)** | No |
| Water vapour | **Sobrino, El Kharraz, and Li (2003)** | Julien et al. (2015) |
| Atmospheric correction | **SMAC (Rahman and Dedieu 1994)** | SMAC (Rahman and Dedieu 1994) |
| BRDF correction | Not yet | Not yet |
| Sea surface temperature | **El Kharraz (2004)** | **Romaguera, Sobrino, and Olesen (2006)** |
| NDVI | **Tucker (1979)** | **Tucker (1979)** |
| Vegetation condition index | **Kogan (1995)** | **Kogan (1995)** |
| Land surface emissivity | **Sobrino, El Kharraz, and Li (2003)** | Romaguera (2004) |
| Land surface temperature | **Sobrino, El Kharraz, and Li (2003)** | **Atitar and Sobrino (2009)** |
| Quicklooks | Yes | Yes |
| Upload to webpage | Yes | Yes |
| Compression | Yes | Yes |
| Upload to server | Yes | Yes |

### 3.1. Preprocessing

The MODIS reception station located at the Global Change Unit of the University of Valencia is equipped with Scanex software, which allows the acquisition and decoding of the image into level 0 data. Indeed, this software package carries out geolocation, calibration (to radiances), and land-, cloud-, and fire-mask building, as stand-alone executable modules from console commands. To that end, two ancillary files must be downloaded regularly from ftp://oceans.gsfc.nasa.gov/COMMON, namely 'utcpole.dat' and 'leapsec.dat'. Therefore, the executable Scanex modules allow for the generation of level 2 products.

However, the MODIS instrument, due to its detector geometry, does not acquire data with exactly identical gain for each detector line, resulting in stripes in the acquired data. To correct this effect, the method presented by Horn and Woodham (1979) is applied. This method (also called cumulative histogram matching) consists of building a specific histogram for each line of detectors for each MODIS acquisition band, which are then intercalibrated and matched to the corresponding band histogram.

Atmospheric correction then has to be implemented only during the daytime for bands 1–7. To that end, the SMAC software (Rahman and Dedieu 1994) was selected. This software is available as both Interactive Data Language (IDL) function and executable. This programme runs on a pixel-by-pixel basis and needs additional information such as (standard values in parentheses): atmosphere type (continental), atmospheric pressure (1013 hPa), aerosol optical thickness (0.05), and ozone concentration (0.33 atm.cm). Additionally, the WV product is needed as an input for the SMAC software. Therefore, the WV product is calculated prior to atmospheric correction.

In regard to thermal channels, the estimation of brightness temperature is required, by inversion of Planck's law:

$$T_i = \frac{c_2/\lambda_{\text{eff}}}{\ln\left(\frac{c_1}{\lambda_{\text{eff}}{}^5 B(T_i)} + 1\right)}, \tag{1}$$

where $T_i$ is the brightness temperature in each thermal band, $c_1 = 1.1491047 \times 10^8$ W m$^{-2}$ sr$^{-1}$ μm$^4$, $c_2 = 1.4387752 \times 10^4$ K μm, $B(T_i)$ is the at-sensor radiance expressed in W m$^{-2}$ sr$^{-1}$ μm$^{-1}$, and $\lambda_{\text{eff}}$ is the effective wavelength (in μm) for each MODIS band $i$.

### 3.2. Near-real-time products

#### 3.2.1. Normalized difference vegetation index

NDVI is estimated as (Tucker 1979)

$$\text{NDVI} = \frac{\rho_2 - \rho_1}{\rho_2 + \rho_1}, \tag{2}$$

where $\rho_1$ and $\rho_2$ correspond to atmospherically corrected reflectances of red and near-infrared MODIS bands 1 and 2, respectively. In our case, NDVI is estimated for daylight acquisitions only.

Table 2. Summary of requirements for MODIS products.

| Product | Bands required | Parameters required | Re-projection | Resolution (m) | Acquisition, estimated size (MB) |
|---|---|---|---|---|---|
| Land mask | Raw data | None | No | 250 | 125 |
| Cloud mask | Raw data | None | No | 250 | 125 |
| Fire mask | Raw data | None | No | 250 | 125 |
| NDVI | 1, 2 | None | No | 250 | 500 |
| FVC | None | NDVI | No | 250 | 500 |
| Emissivity | 1 | NDVI, FVC | Only at night | 250 | 500 |
| Water vapour | 2, 17, 18, 19 | None | Only at night | 1000 | 35 |
| LST | 31, 32 | Emissivity, water vapour | No | 1000 | 35 |
| SST | 31, 32 | None | No | 1000 | 35 |
| BRDF | 1 to 7 | None | Yes | 250 to 500 | 2250 |
| VCI | None | BRDF–NDVI | Yes | 250 | 500 |



### 3.2.2. *Fraction of vegetation cover*

Fraction of vegetation cover (FVC) is estimated from NDVI following Gutman and Ignatov (1998) for daytime acquisitions only as a normalization of NDVI between standard bare soil and dense vegetation values. In the case of MODIS, these values are, respectively, 0.15 and 0.90 (Camacho et al., 2006), and therefore

$$\mathrm{FVC} = \frac{(\mathrm{NDVI}) - 0.15}{0.90 - 0.15}. \tag{3}$$

### 3.2.3. *Emissivity*

Emissivities are estimated for daytime acquisitions from FVC and MODIS band 1 information, following the methodology presented by Sobrino, El Kharraz, and Li (2003). These emissivities correspond to MODIS thermal bands 31 and 32 and are estimated differently depending on the vegetation proportion within a given pixel.

In the case of night-time acquisition, this method cannot be implemented due to the lack of solar radiation and therefore the emissivity estimates during the previous day are re-projected to a latitude/longitude grid, averaged, and re-projected back to the night-time acquisition configuration for further calculations.

These emissivities are expressed as average emissivity $\varepsilon$ (for bands 31 and 32) and spectral difference of emissivities $\Delta\varepsilon$ for different pixel characteristics:

- Vegetation (NDVI > 0.5):

$$e = 0.99\ ;\ \Delta e = 0. \tag{4}$$

- Mixed pixel ($0.2 \leq \mathrm{NDVI} \leq 0.5$):

$$e = 0.971 + 0.018(\mathrm{FVC}); \Delta e = 0.006(1 - (\mathrm{FVC})). \quad (5)$$

- Bare soil (NDVI < 0.2):

$$e = 0.9832 - 0.058\rho_1 \; ; \; \Delta e = 0.0018 - 0.060\rho_1. \quad (6)$$

### 3.2.4. *Water vapour*

WV is estimated using the method developed by Sobrino, El Kharraz, and Li (2003). This method is based on the attenuation of surface-reflected solar radiation and clouds in near-infrared due to WV absorption. To this end, WV-absorbing bands centred at 0.905, 0.936, and 0.94 μm (bands 17, 18, and 19, respectively), in addition to a WV-transparent band centred at 0.865 μm (band 2), are used as follows:

$$W = 0.192W_{17} + 0.453W_{18} + 0.355W_{19}, \quad (7)$$

where

$$W_{17} = 28.449{G_{17}}^2 - 54.434G_{17} + 26.314, \quad (8)$$

$$W_{18} = 27.884{G_{18}}^2 - 23.017G_{18} + 5.012, \quad (9)$$

$$W_{19} = 19.914{G_{19}}^2 - 26.887G_{19} + 9.446, \quad (10)$$

and

$$\begin{aligned} G_{17} &= \frac{L_{17}}{L_2} \\ G_{18} &= \frac{L_{18}}{L_2}, \\ G_{19} &= \frac{L_{19}}{L_2} \end{aligned} \quad (11)$$

where $W$ is atmospheric WV (g cm$^{-2}$) and $L_{17}$, $L_{18}$, $L_{19}$, and $L_2$ are at-sensor radiances (RAD-TOA) of MODIS bands 17, 18, 19, and 2, respectively.

In the case of night-time acquisitions, because this method cannot be implemented due to the lack of solar radiation, WV estimates during the previous day are reprojected to a latitude/longitude grid, averaged, and reprojected back to the night-time acquisition configuration for further calculations.

### 3.2.5. *Land surface temperature*

LST is estimated for day- and night-time acquisitions using the method developed by Sobrino, El Kharraz, and Li (2003):

$$\mathrm{LST} = T_{31} + a_1 + a_2(T_{31} - T_{32}) + a_3(T_{31} - T_{32})^2 + (a_4 + a_5 W)(1 - \varepsilon) + (a_6 + a_7 W)\Delta\varepsilon, \quad (12)$$

where $T_{31}$ and $T_{32}$ are brightness temperatures of MODIS bands 31 and 32, respectively; $\varepsilon$ and $\Delta\varepsilon$ are, respectively, the average emissivity and the spectral emissivity difference of these bands; $W$ is the total WV estimated above; and the coefficients $a_1 = 1.02$, $a_2 = 1.79$, $a_3 = 1.20$, $a_4 = 34.83$, $a_5 = -0.68$, $a_6 = -73.27$, and $a_7 = -5.19$ were determined from simulations (details in Sobrino, El Kharraz, and Li 2003).

#### 3.2.6. Sea surface temperature

SST is estimated for day- and night-time acquisitions using the method developed by El Kharraz (2004):

$$\mathrm{SST} = T_{31} + (b_1 + b_2 W)(T_{31} - T_{32}) + b_3 W + b_4, \quad (13)$$

where $T_{31}$ and $T_{32}$ are brightness temperature of MODIS bands 31 and 32, respectively; $W$ is the total WV estimated above; and the values for $b_1$, $b_2$, $b_3$, and $b_4$ are respectively 1.90, 0.44, 0.05, and 0.34.

### 3.3. Advanced products

#### 3.3.1. Bidirectional reflectance distribution function

Standard BRDF methods use reflectance data from MODIS bands 1–7 over 16 days to estimate BRDF model parameters through least-squares optimization. Here, kernel-driven models are used, these being three-parameter semi-empirical linear models. The theoretical basis of these models is that land surface reflectance is modelled as a sum of three kernels representing basic scattering types: isotropic scattering, radiative transfer-type volumetric scattering as from horizontally homogeneous leaf canopies, and geometric–optical surface scattering as from scenes containing three-dimensional objects that cast shadows and are mutually obscured from view at off-nadir angles:

$$\rho(\theta_s, \theta_v, \phi) = k_0 + k_1 F_1(\theta_s, \theta_v, \phi) + k_2 F_2(\theta_s, \theta_v, \phi), \quad (14)$$

where $\theta_s$ is the Sun zenith angle; $\theta_v$ is the view zenith angle; $\phi$ is the relative azimuth angle; $F_1$ and $F_2$ are the kernels that represent volume scattering and geometric scattering, respectively; and $k_0$, $k_1$, and $k_2$ are the model parameters associated with each kernel. $F_1$ and $F_2$ are fixed functions of the observation geometry derived from physical considerations of radiative transfer at the surface, while $k_0$, $k_1$, and $k_2$ are free parameters estimated on a pixel-by-pixel basis from the data by the least-squares method.

The 'Ross Thick/Li Sparse reciprocal combination', hereafter referred as the Ross–Li model, was selected for the processing of MODIS land-surface measurements (Lucht et al. 2000). The volume-scattering kernel ($F_1$) is based on the Rossthick function derived by Roujean, Leroy, and Deschamps (1992) and modified by Maignan, Bréon, and Lacaze (2004):

$$F_1(\theta_s, \theta_v, \phi) = \frac{4}{3\pi}\frac{1}{\cos\theta_s + \cos\theta_v}\left[\left(\frac{\pi}{2} - \xi\right)\cos\xi + \sin\xi\right]\left(1 + \left(1 + \frac{\xi}{\xi_0}\right)^{-1}\right) - \frac{1}{3}, \tag{15}$$

where $\cos\xi = \cos\theta_s\cos\theta_v + \sin\theta_s\sin\theta_v\cos\phi$ and $\xi_0$ is equal to 1.5°.

The geometric kernel ($F_2$) is based on the LiSparse–Reciprocal model (Li and Strahler 1992) but considering the reciprocal form given by Lucht (1998) that is obtained by the proportions of sunlit and shaded scene components in a scene consisting of randomly located spheroids of height-to-centre-of-crown $h$ and crown vertical to horizontal radius ratio $b/r$:

$$F_2(\theta_s, \theta_v, \phi) = O(\theta_s', \theta_v', \phi) - \sec\theta_s' - \sec\theta_v' + \frac{1}{2}(1 + \cos\xi')\sec\theta_s'\sec\theta_v', \tag{16}$$

where

$$\theta_s' = \arctan\left(\frac{b}{r}\tan\theta_s\right), \text{idem for } \theta_v', \tag{17}$$

$$\cos\xi' = \cos\theta_s'\cos\theta_v' + \sin\theta_s'\sin\theta_v'\cos\phi, \tag{18}$$

$$O(\theta_s', \theta_v', \phi) = \frac{1}{\pi}(t - \sin t\cos t)(\sec\theta_s' + \sec\theta_v'), \tag{19}$$

where $t$ is defined as

$$\cos t = \min\left(1, \frac{h}{b}\frac{\sqrt{D'^2 + (\tan\theta_s'\tan\theta_v'\sin\phi)^2}}{\sec\theta_s' + \sec\theta_v'}\right) \tag{20}$$

and $D'$ as

$$D' = \sqrt{\tan^2\theta_s' + \tan^2\theta_v' - 2\tan\theta_s'\tan\theta_v'\cos\phi}. \tag{21}$$

The dimensionless crown relative height and shape parameters $h/b$ and $b/r$ are within the kernel and should therefore be preselected. For MODIS processing, $h/b = 2$ and $b/r = 1$ (i.e. the spherical crowns are separated from the ground by half their diameter). Generally, the shape of the crowns affects the BRDF more than their relative height.

This BRDF correction is now being investigated in regard to application to the received MODIS data, as presented above or as proposed by Bréon and Vermote (2012), which expresses the above kernel functions for a whole year as a function of NDVI, and allows for a near-real-time estimation of BRDF-corrected data by using the kernel functions estimated for the previous year.

### 3.3.2. *Vegetation condition index*

Similar to FVC, VCI is estimated as a normalization of NDVI between maximum and minimum NDVI values for the considered pixel over a whole year (Kogan 1995):

$$\mathrm{VCI} = \frac{(\mathrm{NDVI}) - (\mathrm{NDVI})_{\min}}{(\mathrm{NDVI})_{\max} - (\mathrm{NDVI})_{\min}}. \quad (21)$$

Therefore, VCI can only be estimated at the end of each year, although a near-real-time estimation could be obtained from near-real-time BRDF-corrected NDVI, by estimating $(\mathrm{NDVI})_{\min}$ and $(\mathrm{NDVI})_{\max}$ values from the BRDF-corrected NDVI for the previous year.

## 4. MSG SEVIRI processing

As stated above, both MODIS and MSG SEVIRI streams of data are processed linearly following a similar scheme (see Table 1). The selected algorithms for MSG SEVIRI processing were also chosen from a literature review, and are based on standard procedures (SMAC atmospheric correction; Rahman and Dedieu 1994) using specific methods described below. Characteristics (resolution, average sample size, etc.) of each of the products described below are presented in Table 3.

### 4.1. Preprocessing

The MSG SEVIRI reception station is equipped with Dartcom software, which allows the acquisition and decoding of the image into level 0 data. Calibration is straightforward, since offset and gain coefficients are included in band metadata. Land/sea mask and observation-viewing zenithal and azimuthal angles are fixed and are available as ancillary files.

Atmospheric correction is then implemented only for pixels under daylight conditions for bands Vis06 and Vis08. To that end, SMAC software (Rahman and Dedieu 1994) was selected and implemented as described in section 3.1, with identical standard values. As in the case of MODIS preprocessing, MSG-SEVIRI WV product is also calculated prior to atmospheric correction.

In regard to thermal channels, the estimation of brightness temperature is required, by inversion of Planck's law (see Equation 1 above).

Table 3. Summary of requirements for MSG SEVIRI products.

| Product | Bands required | Parameters required | Frequency | Image, estimated size (MB) |
|---|---|---|---|---|
| NDVI | Vis06, Vis08 | None | 15 min, 1 day | 26.3 |
| Emissivity | Vis06 | NDVI | 15 min, 1 day | 26.3 |
| Water vapour | Ir108, Ir120 | None | 15 min | 26.3 |
| LST | Ir108, Ir120 | Emissivity, water vapour | 15 min | 26.3 |
| SST | Ir108, Ir120 | None | 15 min | 26.3 |
| BRDF | Vis06, Vis08 | None | 15 min (1 year) | 157.8 |
| VCI | None | BRDF–NDVI | 15 min (1 year) | 26.3 |

### 4.2. Near-real-time products

#### 4.2.1. Normalized difference vegetation index

NDVI is estimated as in Equation (2), but for atmospherically corrected reflectances for MSG SEVIRI bands Vis08 (near-infrared) and Vis06 (red), respectively.

However, NDVI is not expected to change over 24 hours. Therefore, all 15-min NDVI estimates should not vary if not due to changes in the atmosphere (cloud cover) or illumination geometry (since MSG observation geometry is fixed). This property can be used to retrieve BRDF properties.

#### 4.2.2. Emissivity

Emissivities are estimated for daytime acquisitions from NDVI and Vis06 band information, following the threshold method. These emissivities correspond to MSG thermal bands Ir108 and Ir120 and are estimated differently depending on the vegetation proportion within a given pixel.

In the case of night-time acquisition, this method cannot be implemented due to the lack of solar radiation and therefore the emissivity estimates during the previous day are used.

These emissivities are expressed as $\varepsilon_{108}$ and $\varepsilon_{120}$ for different pixel characteristics:

- Vegetation (NDVI > 0.5):

$$\varepsilon_{108} = 0.99;\ \varepsilon_{120} = 0.99. \tag{22}$$

- Mixed pixel ($0.2 \leq \text{NDVI} \leq 0.5$):

$$\varepsilon_{108} = 0.968 + 0.021(\text{PV});\ \varepsilon_{120} = 0.976 + 0.015(\text{PV}). \tag{23}$$

- Bare soil (NDVI < 0.2):

$$\varepsilon_{108} = 0.977 - 0.048\rho_{\text{Vis06}};\ \varepsilon_{120} = 0.981 - 0.026\rho_{\text{Vis06}}. \tag{24}$$

where $\rho_{\text{band}}$ is the atmospherically corrected reflectance for MSG SEVIRI bands (bands = Vis06, Vis08) and PV is the proportion of vegetation within the pixel, estimated as

$$\text{PV} = \frac{((\text{NDVI}) - 0.2)^2}{0.09}. \tag{25}$$

#### 4.2.3. Water vapour

A first approach for estimating WV was based on the method developed by Sobrino and Romaguera (2008). However, due to the complex application of this algorithm to near-real-time processing, a novel instantaneous approach was designed (Julien et al. 2015) and is presented briefly below:

$$W = w_0 + w_1 T_{062}(T_{108} - T_{120}), \tag{26}$$

where $T_{108}$ and $T_{120}$ are brightness temperatures of MSG bands Ir108 and Ir120, respectively, and $T_{062}$ is the brightness temperature of the MSG SEVIRI water absorption band at 6.2 μm (Wv062). Values for coefficients $w_0$ and $w_1$ are, respectively, 1.4 g cm$^{-2}$ and 0.00692 g cm$^{-2}$ K$^{-1}$.

#### 4.2.4. Land surface temperature

LST is estimated for day- and night-time acquisitions using the method developed by Atitar and Sobrino (2009):

$$\begin{aligned} \mathrm{LST} = T_{108} &+ \left[1.34 - \frac{0.11}{\cos^2\theta}\right](T_{108} - T_{120}) + \left[0.29 + \frac{0.08}{\cos^2\theta}\right](T_{108} - T_{120})^2 \\ &+ \left[60.67 - \frac{10.01}{\cos^2\theta}\right](1 - \varepsilon) + \left[-6.71 + \frac{2.47}{\cos^2\theta}\right] W(1 - \varepsilon) \\ &+ \left[-125.91 + \frac{15.09}{\cos^2\theta}\right]\Delta\varepsilon + \left[19.44 - \frac{4.27}{\cos^2\theta}\right] W\Delta\varepsilon + \left[-0.44 + \frac{0.57}{\cos^2\theta}\right] \end{aligned}, \tag{27}$$

where $T_{108}$ and $T_{120}$ are brightness temperatures of MSG bands Ir108 and Ir120, respectively; $\varepsilon$ and $\Delta\varepsilon$ are, respectively, the average emissivity and the spectral emissivity difference of these bands; $W$ is the total WV estimated above; and $\theta$ is the observation zenith angle.

#### 4.2.5. SST

SST is estimated for day- and night-time acquisitions using the method developed by Romaguera, Sobrino, and Olesen (2006):

$$\begin{aligned} \mathrm{SST} = T_{108} &+ (0.99\cos\theta + 0.21)(T_{108} - T_{120}) \\ &+ \left(\frac{0.364}{\cos\theta} + 0.15\right)(T_{108} - T_{120})^2 + \frac{0.327}{\cos^2\theta} + 0.11 \end{aligned}, \tag{28}$$

where $T_{108}$ and $T_{120}$ are brightness temperatures of MSG bands Ir108 and Ir120, respectively, and $\theta$ is the observation zenith angle.

### 4.3. Advanced products

#### 4.3.1. Bidirectional reflectance distribution function

The approach for BRDF-corrected MSG SEVIRI data (Vis06 and Vis08) is the same as that for MODIS data (see above), and is currently being implemented. However, in the case of MSG data, since the observation angle is fixed by the geostationary characteristic of its associated platform, only the normalization of illumination can be carried out directly from MSG data. Approaches exist to normalize observations to illumination and observation nadir, although additional data are needed (e.g. from MODIS sensor). Here we prefer MSG-only processing, since it is easier to implement and does not hinder the time-series analysis of MSG data, because the observations will be normalized to a

standard observation and illumination geometry, consisting of the observation angle for each pixel and nadir illumination. Therefore, the BRDF correction will only consider differences in pixel illumination.

#### 4.3.2. Vegetation condition index

MSG SEVIRI VCI is estimated following the same approach as described above for MODIS VCI. NDVI minimum and maximum values are estimated after time-series reconstruction using the iterative interpolation for data reconstruction (IDR) approach (Julien and Sobrino 2010) as implemented in Sobrino, Julien, and Soria (2013) for the previous year, and estimated immediately after image reception, screening out values for which the NDVI increase over the previous 24 hours is within a pixel-specific threshold as determined from NDVI temporal behaviour analysis for the previous year. Therefore, the VCI-estimated data are incremental, updated at each image acquisition for cloud-free pixels.

## 5. Applications

With the availability of such a huge amount of data, countless applications can be carried out, from vegetation monitoring and forecasting to disaster early-warning. Hereafter, we present two among these applications, focused on the one hand on hot spot detection and on the other hand on phenology monitoring. Finally, the geo-portal for the download of the products presented above is briefly presented.

### 5.1 Hot spot detection

Forest fires are a considerable danger to human health, through corporal and property damage as well as air contamination, and play a key role in the carbon cycle through the emission of $CO_2$, a gas which has been evidenced as a major contributor to global warming. As regards spectral information, forest fires (and fires in general) present temperatures in the mid-wave infrared (MIR) and thermal infrared (TIR) region higher than their surroundings, which allows for their detection from remote sensors such as MODIS (Giglio et al. 2003) and MSG SEVIRI (Calle, Casanova, and Romo 2006). In Table 4, we present a sample of four hot spots detected in Portugal from MSG SEVIRI acquisition on 2 September 2014 at 17:45 (UTC), along with the estimated characteristics of the detected fire (fire radiative power (FRP), fire temperature, and burning area). The system is configured so that alert emails are sent to warn of forest fires in southwestern Europe as soon as they are detected (within 5 min of the end of image reception) from either MSG SEVIRI or MODIS instruments.

Table 4. Coordinates and characteristics of the fire detected from MSG SEVIRI acquisition on 2 September 2014 at 17:45 (UTC).

| Pixel | Latitude (º) | Longitude (º) | Fire radiative power (MW) | Temperature (K) | Area (ha) |
|---|---|---|---|---|---|
| 1 | 40.69 | −6.89 | 19.7 | 1194 | 0.24 |
| 2 | 40.69 | −6.85 | 28.5 | 932 | 0.87 |
| 3 | 40.25 | −7.73 | 34.1 | 1495 | 0.22 |
| 4 | 40.25 | −7.69 | 32.0 | 1857 | 0.12 |

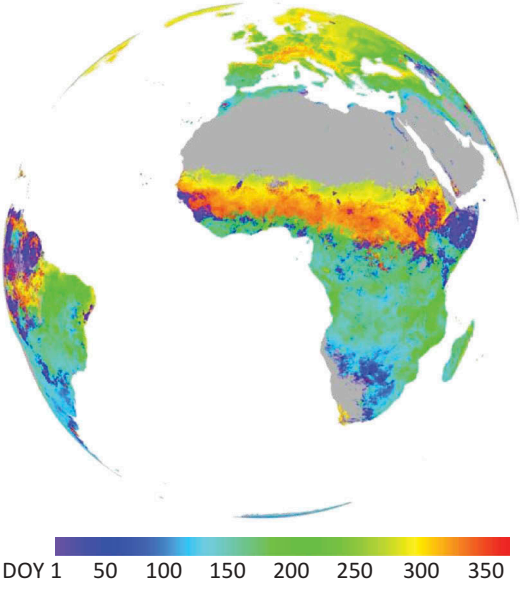


Figure 2. End of season (EOS) dates for 2013 as retrieved from MSG SEVIRI NDVI time series.

### 5.2 *Phenology estimation*

Monitoring NDVI throughout a complete year allows for the estimation of phenological phases, such as the dates corresponding to the start and end of the season (SOS and EOS, respectively). This information is of utmost importance since both dates play a role in water and carbon cycles, in direct relation to climate warming prediction, and are a known indicator of climate change through plant sensitivity to temperatures. In Figure 2 we present an example of EOS dates for 2013 for the entire MSG SEVIRI disc. To that end, instantaneous NDVI values at 12:00 UTC have been cloud-corrected and gap-filled through the procedure described in Sobrino, Julien, and Soria (2013) and then analysed for yearly cycle characterization. Direct comparison to independent PEP725 ground station data showed an error below 1 week for EOS in Europe (Sobrino, Julien, and Soria 2013).

### 5.3 *Geo-portal*

All products shown in bold in Table 1 are available for download for registered users (registration upon request) from the geo-portal located at http://ceosspain.lpi.uv.es. Guest users can browse the available data, although without permission to download. The architecture of the geo-portal is described thoroughly in Sevilla et al. (2015), and allows for the search of the entire database (since mid-2007) for user-defined specific locations and acceptable cloud contamination levels in the case of MODIS data, while MSG SEVIRI data are provided for the entire observation disc only. This geo-portal is presented in Figure 3.


Figure 3. Overview of the geo-portal from which all MODIS and SEVIRI products since 2007 can be downloaded (http://ceosspain.lpi.uv.es). Red rectangle corresponds to the area selected (Iberian Peninsula) for database exploration.

## 6. Conclusion

The MODIS and MSG SEVIRI receiving stations at the Global Change Unit of the University of Valencia have been operational since mid-2007. All received data were processed as described above, allowing for specific applications such as fire hot spot detection, phenology monitoring, and temperature spatial homogeneity studies (not described here). These data are available for download to the scientific community and the general public from the geo-portal on the CEOS-SPAIN webpage: http://ceosspain.lpi.uv.es. Additional products (BRDF correction) will be added in the near future, and products presented will be validated from multitemporal data recorded at various ground stations in Spain, representative of various land covers and land uses. Finally, the available parameters will be extended to the Suomi National Polar-orbiting Partnership Visible Infrared Imaging Radiometer Suite instrument, from which data are already being received at our station.

## Acknowledgement

The authors are grateful to all members of the Global Change Unit of the University of Valencia for their dedication in keeping the MSG and MODIS receiving station running over the years.

## Disclosure statement

No potential conflict of interest was reported by the authors.

## Funding

This work was supported by the Spanish Ministerio de Ciencia y Tecnología [CEOS-SPAIN, project AYA2011-29334-C02-01].

## References

Ackerman, F., L. Strabala, B. Gumley, and P. Menzel 2010. "Discriminating Clear-Sky from Cloud with MODIS - Algorithm Theoretical Basis Document." Products: MOD35. ATBD Reference Number: ATBD-MOD-06.

Atitar, M., and J. A. Sobrino. 2009. "A Split-Window Algorithm for Estimating LST from Meteosat 9 Data: Test and Comparison with in Situ Data and MODIS LST." *IEEE Geoscience and Remote Sensing Letters* 6 (1): 122–126. doi:10.1109/LGRS.2008.2006410.

Bréon, F.-M., and E. Vermote. 2012. "Correction of MODIS Surface Reflectance Time Series for BRDF Effects." *Remote Sensing of Environment* 125: 1–9. doi:10.1016/j.rse.2012.06.025.

Calle, A., J. L. Casanova, and A. Romo. 2006. "Fire Detection and Monitoring Using MSG Spinning Enhanced Visible and Infrared Imager (SEVIRI) Data." *Journal of Geophysical Research: Biogeosciences* 111 (G4): G04S06. doi:10.1029/2005JG000116.

Camacho De Coca, F., J.-C. Jiménez-Muñoz, B. Martínez, P. Bicheron, R. Lacaze, and M. Leroy, 2006. "Prototyping of Fcover Product over Africa Based on Existing CYCLOPES and JRC Products for Vgt4africa." Proceedings of the 2nd RAQRS Symposium, edited by J. A. Sobrino, Torrent, September 22–25, 722–727.

El Kharraz, J., 2004. "*Determinación De La Temperatura De La Superficie Terrestre a Partir De Datos MODIS*." PhD diss., University of Valencia, Spain.

Giglio, L., J. Descloitres, C. O. Justice, and Y. Kaufman. 2003. "An Enhanced Contextual Fire Detection Algorithm for MODIS." *Remote Sensing of Environment* 87: 273–282. doi:10.1016/S0034-4257(03)00184-6.

Gutman, G., and A. Ignatov. 1998. "The Derivation of the Green Vegetation Fraction from NOAA/AVHRR Data for Use in Numerical Weather Prediction Models." *International Journal of Remote Sensing* 19 (8): 1533–1543. doi:10.1080/014311698215333.

Horn, B. K. P., and R. J. Woodham. 1979. "Destriping LANDSAT MSS Images by Histogram Modification." *Computer Graphics and Image Processing* 10 (1): 69–83. doi:10.1016/0146-664X(79)90035-2.

Julien, Y., and J. A. Sobrino. 2010. "Comparison of Cloud-Reconstruction Methods for Time Series of Composite NDVI Data." *Remote Sensing of Environment* 114 (3): 618–625. doi:10.1016/j.rse.2009.11.001.

Julien, Y., J. A. Sobrino, C. Mattar, and J.-C. Jiménez-Muñoz. 2015. "Near Real-Time Estimation of WV Column from MSG SEVIRI Thermal Infrared Bands: Implications for Land Surface Temperature Retrieval." *IEEE Transactions on Geoscience and Remote Sensing* 53 (8): 4231–4237.

Kogan, F. N. 1995. "Droughts of the Late 1980s in the United States as Derived from NOAA Polar-Orbiting Satellite Data." *Bulletin of the American Meteorological Society*, 76 (5): 655–668. doi:10.1175/1520-0477(1995)076<0655:DOTLIT>2.0.CO;2.

Li, X., and A. H. Strahler. 1992. "Geometric-Optical Bidirectional Reflectance Modeling of the Discrete Crown Vegetation Canopy: Effect of Crown Shape and Mutual Shadowing." *IEEE Transactions on Geosience and Remote Sensing* 30: 276–292.

Lucht, W. 1998. "Expected Retrieval Accuracies of Bidirectional Reflectance and Albedo from EOS-MODIS and MISR Angular Sampling." *Journal of Geophysical Research-Atmospheres* 103: 8763–8778.

Lucht, W., A. H. Hyman, A. H. Strahler, M. J. Barnsley, P. Hobson, and J.-P. Muller. 2000. "A Comparison of Satellite-Derived Spectral Albedos to Ground-Based Broadband Albedo Measurements Modeled to Satellite Spatial Scale for A Semidesert Landscape." *Remote Sensing of Environment* 74: 85–98. doi:10.1016/S0034-4257(00)00125-5.

Maignan, F., F.-M. Bréon, and R. Lacaze. 2004. "Bidirectional Reflectance of Earth Targets: Evaluation of Analytical Models Using a Large Set of Spaceborne Measurements with Emphasis on the Hot Spot." *Remote Sensing of Environment* 90: 210–220. doi:10.1016/j.rse.2003.12.006.

Rahman, H., and G. Dedieu 1994. "SMAC: A Simplified Method for the Atmospheric Correction of Satellite Measurements in the Solar Spectrum." *International Journal of Remote Sensing* 15 (1): 123–143. doi:10.1080/01431169408954055.

Romaguera, M., 2004. "Determinació De La Temperatura De La Superficie Terrestre a Partir De Dades MSG1/SEVIRI." DEA Research Report, University of Valencia, Spain.

Romaguera, M., J. A. Sobrino, and F.-S. Olesen. 2006. "Estimation of Sea Surface Temperature from SEVIRI Data: Algorithm Testing and Comparison with AVHRR Products." *International Journal of Remote Sensing* 27: 5081–5086. doi:10.1080/01431160500165674.

Roujean, J. L., M. Leroy, and P. Y. Deschamps. 1992. "A Bidirectional Reflectance Model of the Earths Surface for the Correction of Remote-Sensing Data." *Journal of Geophysical Research-Atmospheres* 97: 20455–20468.

Sevilla, J., Y. Julien, G. Soria, J. A. Sobrino, and A. Plaza. 2015. "A New Geo-Portal for MODIS/SEVIRI Image Products with Geolocation-Based Retrieval Functionality." *Journal of Applied Remote Sensing* 9: 096079. doi:10.1117/1.JRS.9.096079.

Sobrino, J. A., J. El Kharraz, and Z.-L. Li. 2003. "Surface Temperature and Water Vapour Retrieval from MODIS Data." *International Journal of Remote Sensing* 24: 5161–5182. doi:10.1080/0143116031000102502.

Sobrino, J. A., Y. Julien, and G. Soria. 2013. "Phenology Estimation From Meteosat Second Generation Data." *IEEE Journal of Selected Topics in Applied Earth Observations and Remote Sensing* 6 (3): 1653–1659. doi:10.1109/JSTARS.2013.2259577.

Sobrino, J. A., and M. Romaguera. 2008. "Water-Vapour Retrieval from Meteosat 8/SEVIRI Observations." *International Journal of Remote Sensing* 29 (3): 741–754. doi:10.1080/01431160701311267.

Tucker, C. J. 1979. "Red and Photographic Infrared Linear Combinations for Monitoring Vegetation." *Remote Sensing of Environment* 8 (2): 127–150. doi:10.1016/0034-4257(79)90013-0.